COMMUNICATIONS IN NUMERICAL METHODS IN ENGINEERING
Commun. Numer. Meth. Engng 2008; **24**:671–681
Published online 5 January 2007 in Wiley InterScience (www.interscience.wiley.com). DOI: 10.1002/cnm.980

A multigrid method for solving the Navier–Stokes/Boussinesq equations

Nader Ben Cheikh*, †, Brahim Ben Beya and Taieb Lili

Laboratoire de mécanique des fluides, Département de Physique, Faculté des sciences de Tunis El-manar, 1060 Tunis, Tunisia

SUMMARY

The present work investigates the efficiency and the accuracy of a multigrid (MG) technique for solving the Navier–Stokes/Boussinesq equations. In order to improve convergence, an accelerated full multigrid (AFMG) method with the iterative red and black successive over-relaxation smoother (RBSOR) is utilized. The AFMG method consists in introducing an accelerated parameter $\Gamma>0$ in the standard full multigrid procedure (FMG). A well-known benchmark problem is used to demonstrate the effectiveness and the accuracy of the method. Solutions are compared with those of the literature and show excellent agreement. Results for Prandtl numbers $Pr = 12.5$, 6.8, 0.71 and 0.025 are also presented in this paper. It is observed that the mean heat transfer rate is minimum for $Pr = 0.71$ and maximum for $Pr = 0.025$. Copyright © 2007 John Wiley & Sons, Ltd.

Received 1 July 2006; Revised 1 November 2006; Accepted 30 November 2006

KEY WORDS: finite-volume; multigrid; natural convection; projection method

1. INTRODUCTION

The application of computational fluid dynamics (CFD) methods in engineering problems shows that for sufficient accuracy, large grid sizes are needed for capturing thin boundary layer properties, detecting high heat transfer spots or resolving small eddy regions. On relatively fine grids, standard single-grid iterative methods suffer unfortunately from poor convergence characteristics. The reason is that iterative methods can efficiently smooth out only those Fourier error components of wavelengths smaller than or comparable to the grid size. In contrast, multigrid (MG) methods aim at covering a wider spectrum of wavelengths through relaxation on various grids [1]. The applications of MG methods to solve elliptic partial differentiation equations iteratively have shown practically optimum convergence characteristics [2–4]. The computation times are directly proportional to the number of grid points, allowing very fine grids to be used.

*Correspondence to: Nader Ben Cheikh, Laboratoire de mécanique des fluides, Département de Physique, Faculté des sciences de Tunis El-manar, 1060 Tunis, Tunisia.
†E-mail: nader_bc@yahoo.fr

In this paper a finite volume, full multigrid method (FMG) applied to natural convection flows is presented. The smoother used in the FMG procedure is the iterative red and black successive over-relaxation scheme (RBSOR). In order to accelerate convergence, an acceleration factor is implemented yielding to the accelerated full multigrid (AFMG) procedure [5, 6].

In the next section the numerical approach is briefly described, followed by the description of the RBSOR scheme and the AFMG method. Next, the implementation of the AFMG algorithm is validated by a relatively recent CFD benchmark problem: a time-dependent buoyancy-driven flow in a tall cavity with aspect ratio 8:1 [7]. Results related to different Prandtl numbers are also presented. In the final section the most important findings of this study are summarized.

2. NUMERICAL APPROACH

The non-dimensional governing equations for an incompressible flow, corresponding to the continuity, Navier–Stokes and energy equations, under the Boussinesq approximation, are given by

$$\frac{\partial u_i}{\partial x_i} = 0 \tag{1}$$

$$\frac{\partial u_i}{\partial t} + \frac{\partial (u_j u_i)}{\partial x_j} = -\frac{\partial p}{\partial x_i} + \sqrt{\frac{Pr}{Ra}} \frac{\partial^2 u_i}{\partial x_j \partial x_j} + \theta \delta_{i2} \tag{2}$$

and

$$\frac{\partial \theta}{\partial t} + \frac{\partial (u_i \theta)}{\partial x_i} = \frac{1}{\sqrt{Ra\, Pr}} \frac{\partial^2 \theta}{\partial x_i \partial x_i} \quad (i = 1, 2) \tag{3}$$

where $u_i = (u, v)$, p and θ are the velocity, the kinematic pressure and temperature, respectively. Here δ_{ij} is the Krönecker symbol. The non-dimensional parameters are Rayleigh number (Ra) and Prandtl number (Pr) defined as $Ra = g\beta \Delta T W^3 / \nu\alpha$ and $Pr = \nu/\alpha$, where ν is the kinematic viscosity, α the thermal diffusivity, W the characteristic length, g the gravitational acceleration, β the isobaric coefficient of thermal expansion and $\Delta T = T_h - T_c$ the temperature difference between the hot and cold walls.

The unsteady Navier–Stokes and energy equations are discretized by a second-order time stepping of finite difference type. Non-linear terms in Equation (2) are treated explicitly with a second-order Adams–Bashforth scheme. Convective terms in Equation (3) are treated semi-implicitly and diffusion terms in both Equations (2) and (3) are treated implicitly. Note that the advective terms in Equation (2) are discretized using a QUICK third-order scheme [8], while a second-order central differencing scheme is used to discretize advective terms in energy equation (3). A finite-volume method [6] is used to discretize the Navier–Stokes and energy equations. In order to get round the difficulty that resides in the strong velocity–pressure coupling, we choose to use a projection method [9, 10]. Equations to solve are the equation of energy, the equation related to an intermediate velocity field and a Poisson pressure correction equation. The two first equations are solved using the red and black successive over-relaxation method (RBSOR), while the Poisson equation is solved using an AFMG.

DOI: 10.1002/cnm

3. ACCELERATED FULL MULTIGRID METHOD

3.1. RBSOR scheme

The successive over-relaxation method (SOR) is a method of solving a linear system of equations derived by extrapolating the Gauss–Seidel method. One SOR iteration permits to find a new approximation of the solution $X_{i,j}^{\text{new}}$ on node (i, j) by knowing the approximation $X_{i,j}^{\text{old}}$ of the previous iteration

$$X_{i,j}^{\text{new}} = X_{i,j}^{\text{old}} - \omega \frac{R_{i,j}}{a_P} \tag{4}$$

Here, ω is the relaxation parameter and $R_{i,j}$ is the residual term defined as

$$R_{i,j} = a_W X_{i-1,j}^{\text{new}} + a_S X_{i,j-1}^{\text{new}} + a_P X_{i,j}^{\text{old}} + a_E X_{i+1,j}^{\text{old}} + a_N X_{i,j+1}^{\text{old}} - Sc_{i,j} \tag{5}$$

where Sc is the source term and W, E, S and N are the four immediate neighbours of point P on node (i, j).

By combining the two techniques red–black ordering and successive over-relaxation one can significantly improve the rate of convergence. The algorithm divides the unknowns into two groups: red and black (sometimes called odd and even). With red–black ordering, the equation system is divided into alternating red and black points in a checkerboard fashion as shown in Figure 1. The red–black SOR method consists, in a typical iteration, to perform in a first step an update on all red cells. The second step consists to update the remaining black cells, by using the red cells that have just been updated.

3.2. AFMG method

The main idea of the multigrid method can be understood by considering the simplest case of a two-grid method. Suppose we are trying to solve the linear elliptic Poisson equation:

$$\Delta \phi_k = S_k \tag{6}$$

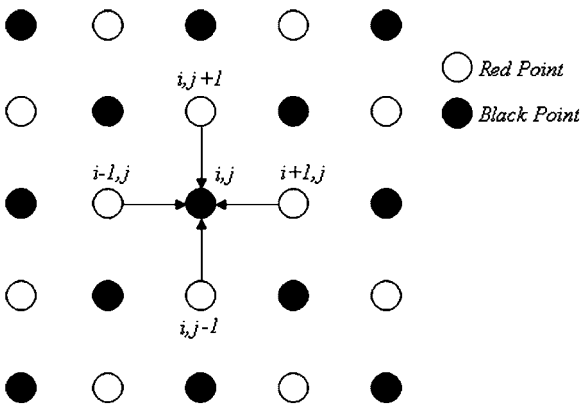

Figure 1. Red–black checker-pointing for SOR.

DOI: 10.1002/cnm

where S_k is the source term, ϕ_k the exact solution and k the grid level. Note that level 1 corresponds to the coarsest grid and level k to the finest mesh.

After η_k^{pre} RBSOR pre-smoothing iterations with a relaxation factor ω_k^{pre} applied to (6) one obtains an intermediate value $\tilde{\phi}_k$ satisfying

$$\Delta\tilde{\phi}_k - S_k = R_k \tag{7}$$

where R_k is the corresponding residual. Substituting (6) in (7) one gets

$$\Delta(\tilde{\phi}_k - \phi_k) = R_k \tag{8}$$

Here $(\tilde{\phi}_k - \phi_k)$ is the error or the correction in $\tilde{\phi}_k$. Equation (8) can then be rewritten as

$$\Delta\psi_k = R_k \tag{9}$$

So, the exact solution $\psi_k = \tilde{\phi}_k - \phi_k$ permits one to determine the exact ϕ_k field by the following correction:

$$\phi_k = \tilde{\phi}_k - \psi_k \tag{10}$$

The multigrid method consists of determining the correction field ψ_k on the coarser grid $k-1$. For that purpose only the residual R_k is transferred from grid k to grid $k-1$. This interpolation is obtained by a restriction operator I_k^{k-1}. Thus, on grid $k-1$, we solve

$$\Delta\phi_{k-1} = I_k^{k-1}(R_k) \tag{11}$$

The above equation is solved with the iterative RBSOR method (η_{k-1}^{pre} iterations and a relaxation parameter $\omega_{k-1}^{\text{pre}}$). The obtained field ϕ_{k-1} is thereafter interpolated toward the grid k by the intermediary of a prolongation operator I_{k-1}^k. After η_{k-1}^{post} RBSOR post-smoothing iterations ($\omega = \omega_{k-1}^{\text{post}}$) of equation

$$\Delta I_{k-1}^k(\phi_{k-1}) = R_k \tag{12}$$

the obtained field is injected in ψ_k and the new field ϕ_k^{new} is updated by the relation

$$\phi_k^{\text{new}} = \tilde{\phi}_k - \psi_k \tag{13}$$

The method outlined above describes one V-cycle on two grids. Generally more than two grids are employed. In that case, after η_{k-1}^{pre} RBSOR iterations ($\omega = \omega_{k-1}^{\text{pre}}$) on grid $k-1$, an approximate solution $\tilde{\phi}_{k-1}$ is obtained and the residue R_{k-1} is transferred to the coarser grid $k-2$ and so on. When the coarsest grid is reached, the reverse procedure starts, in which corrections are evaluated and transferred to the finer grid. The exact solution ϕ_1 is calculated on the coarsest grid and extrapolated to grid 2. After η_2^{post} iterations (with a relaxation factor ω_2^{post}) of the prolongated field we obtain the correction to add to the prevailing approximate solution $\tilde{\phi}_2$, and so on, until reaching the finest grid.

We have implemented our multigrid procedure in a so-called full multigrid (FMG) fashion [2]. Indeed, before starting V-cycles, the source term is calculated on the coarsest grid permitting the determination of an exact solution ϕ_1. This solution is progressively interpolated from the coarsest to the finest grid, and used there as a starting guess for the V-cycle procedure (see Figure 2).

DOI: 10.1002/cnm

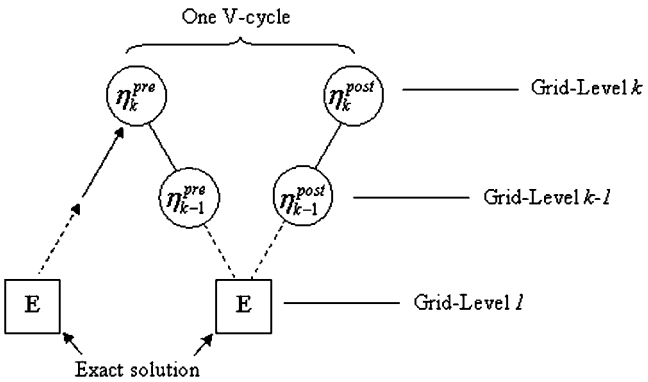

Figure 2. Schematic presentation of the FMG procedure.

The convergence of the result is established when the residue R_k on the finest grid becomes lower than 10^{-6}.

In order to optimize the number of V-cycles, it is demonstrated [6] that convergence can be substantially improved by just multiplying the correction field in the MG procedure by some suitable factor $\Gamma > 0$ (AFMG method)

$$\phi_k^{\text{new}} = \tilde{\phi}_k - \Gamma \psi_k \tag{14}$$

The chosen value of Γ is discussed in the next paragraph.

4. RESULTS AND DISCUSSION

4.1. Numerical validation

In June 2001, a special session dedicated to understanding the fluid dynamics of a differentially heated cavity of aspect ratio $A = 8$ was held at the First MIT Conference on Computational Fluid and Solid Mechanics [7]. The primary objective for this special session was to identify the correct, i.e. best time-dependent benchmark solution for the 8:1 thermally driven cavity at particular values of Rayleigh and Prandtl numbers. As a test case, we consider this benchmark problem to validate our code. Thus, in this paragraph, results related to $Ra = 3.4 \times 10^5$, $Pr = 0.71$ and an aspect ratio $A = 8$ are presented. The number of control volumes applied on the finest grid are 96×480 corresponding to six levels in the multigrid calculation. The coarsest grid level consisted of 3×15 number of control volumes. The number of smoothing sweeps ($\eta_k^{\text{pre}}, \eta_k^{\text{post}}$) and the relaxation factors ($\omega_k^{\text{pre}}, \omega_k^{\text{post}}$) on each grid level k are summarized in Table I. Grids are uniform in the vertical direction and non-uniform in the horizontal direction with smallest cells near hot and cold walls. Note that the grids are obtained with Cartesian meshes.

We ran our computations on three different grids with increasing refinement: 24×120 nodes (coarse), 48×240 nodes (medium) and 96×480 nodes (fine). Preliminary tests on grid 24×120 have been carried to determine an optimal value of factor Γ. A mean value of $\Gamma = 3.75$ were retained. Figure 3 shows time histories of V-cycles for $\Gamma = 1$ (classical FMG) and $\Gamma = 3.75$ (AFMG). It clearly appears that the AFMG method reduces in a significant manner the number

DOI: 10.1002/cnm

Table I. Smoothing sweeps and over-relaxation factors used for the 8:1 differentially heated problem.

Grid level	Grid size	ω^{pre}	ω^{post}	η^{pre}	η^{post}
6	96×480	1.9	1.0	1	2
5	48×240	1.9	0.1	3	1
4	24×120	1.9	0.1	3	1
3	12×60	1.9	0.1	3	1
2	6×30	1.9	0.1	3	1
1	3×15	1.6	1.6	—	—

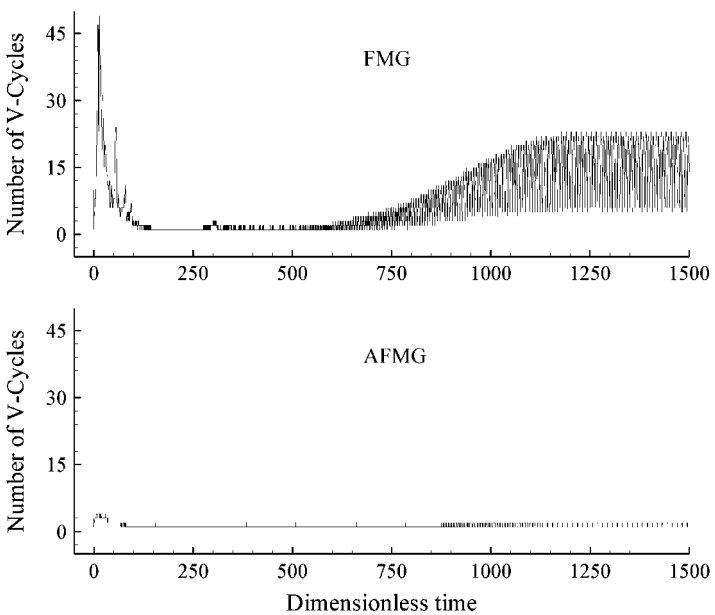

Figure 3. Time history of V-cycles performed with FMG and AFMG.

of V-cycles. Hence, a value of $\Gamma = 3.75$ was kept for computations on all grids. Calculations have been carried until a non-dimensional time of $t = 1500$.

During the flow solution, time history data at point 1 of co-ordinate $(x, y) = (0.1810, 7.3700)$ (see Reference [7] for details) were reported at each time step. Table II provides a summary of the time-history data for the three grid resolutions. The time averaged value is given along with the amplitude of the oscillations for each variable presented in the table. The time average was integrated over 10 complete time periods near the end of the calculation. The table presents information at point 1 for the velocity in the x-direction (u_1), the velocity in the y-direction (v_1), the temperature (θ_1) and the Nusselt number (Nu). The corresponding fluctuating x-velocity, y-velocity, temperature and Nusselt number are Δu_1, Δv_1, $\Delta\theta_1$ and ΔNu. The period, τ_θ, is the period associated with the temperature oscillation at point 1. In order to assess the comparative performance of the present results to the benchmark test, Nu, ΔNu and τ_θ are shown in Table III

DOI: 10.1002/cnm

Table II. Numerical results at Point 1 ($x = 0.1810$, $y = 7.3700$) on different grids.

Quantity	Grid resolution		
	24×120	48×240	96×480
u_1	5.01203×10^{-2}	5.37072×10^{-2}	5.61780×10^{-2}
Δu_1	7.16083×10^{-4}	3.59755×10^{-2}	5.43379×10^{-2}
v_1	4.52762×10^{-1}	4.59891×10^{-1}	4.61412×10^{-1}
Δv_1	1.12033×10^{-3}	5.28620×10^{-2}	7.67392×10^{-2}
θ_1	2.68107×10^{-1}	2.66011×10^{-1}	2.65582×10^{-1}
$\Delta\theta_1$	5.93518×10^{-4}	2.88141×10^{-2}	4.26336×10^{-2}
Nu	4.61383	4.58802	4.58179
ΔNu	1.70366×10^{-4}	4.98058×10^{-3}	7.10453×10^{-3}
τ_θ	3.7440	3.4400	3.4160

Table III. Comparison of benchmark solutions with some contributors to the MIT session held in June 2001.

First author [7]	Nu	ΔNu	τ_θ
Johnston	4.56700	0.007130	3.4220
Davis	4.57960	0.007000	3.4120
LeQuéré	4.57946	0.007100	3.4115
Westerberg	4.58700	0.007600	3.4100
Present study	4.58179	0.007104	3.4160

Table IV. Grid sizes and the corresponding execution times.

Grid size	Δt	Steps	Method	Total CPU (s)	CPU (s)/step
12×120	0.032	46 875	AFMG	702	0.015
			RBSOR	12 636	0.27
48×240	0.016	93 750	AFMG	8296	0.088
			RBSOR	605 474	6.46
96×480	0.008	187 500	AFMG	63 355	0.338
			RBSOR	15 930 000*	84.96

*Estimated.

and compared with some of the contributors to the MIT session. Our presented results have been calculated on a grid 96×480 for $1465.84 \leqslant t \leqslant 1500$ (10 periods) and show good agreement with those of the available literature.

4.2. Time performances

The CPU times, measured on a Dell Dimension 4600 system with a single 2.9 GHz processor (specFP95 = 71), corresponding to RBSOR and AFMG methods are compared in Table IV. The improvement factors in execution time, when comparing the single grid and the MG algorithm,

DOI: 10.1002/cnm

Table V. Comparison of the normalized algorithm timing metric η_{AT}.

First author [7]	η_{AT}	Ranking
Johnston	1.00	1/(26)
Christon II	1.31	2/(26)
Christon III	1.35	3/(26)
Present study	2.11	4/(26)
Matsumoto	2.34	5/(26)
Bruneau	3.40	6/(26)
Chan I	12.77	10/(26)
LeQuéré	90.17	24/(26)
Ingberg	2010.14	26/(26)

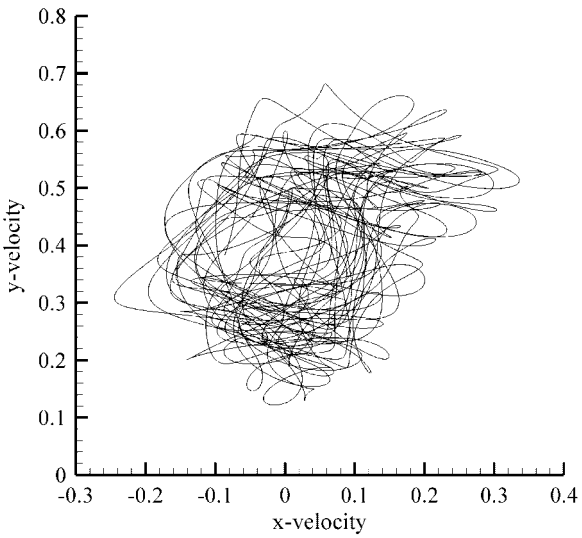

Figure 4. Phase portrait for $Pr = 0.025$ on grid 96×480 at point 1.

are of 18, 73 and 251 for grids 12×120, 48×240 and 96×480, respectively. By introducing the factor γ

$$\gamma = \frac{\mathrm{CPU_{FMG}}}{\mathrm{CPU_{AFMG}}}$$

which represents the improvement factor in execution time between FMG and AFMG method, a value of $\gamma = 1.74$ was obtained. In order to reflect the computational cost required to obtain the solution of the benchmark problem, a normalized algorithm timing has been developed [7] and is defined as

$$\eta_{AT} = \left(\frac{\mathrm{ms}}{\mathrm{node} \cdot \mathrm{step}} \cdot \frac{\mathrm{steps}}{\mathrm{period}} \right) \cdot \mathrm{specFP95}$$

DOI: 10.1002/cnm

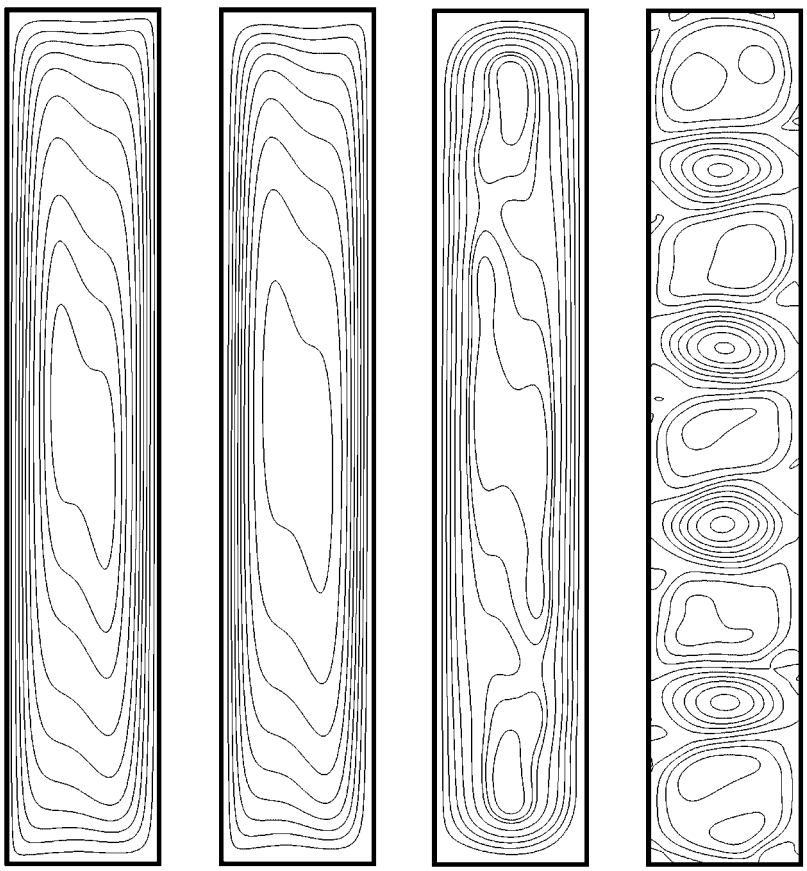

Figure 5. Streamlines for decreasing Prandtl numbers on grid 96×480: (a) $Pr = 12.5$; (b) $Pr = 6.8$; (c) $Pr = 0.71$; and (d) $Pr = 0.025$.

The normalized performance metric is scaled in a relative sense so that the minimum value of η_{AT} is unity. The normalized performance metric is presented in Table V and compared with some of the contributors to the MIT session. Our metric is ranked fourth and shows that the numerical method presented in this paper is sufficiently fast to study natural convection problems on relatively fine grids in acceptable CPU times.

4.3. Effect of Prandtl number

In this section, results for higher and lower Prandtl numbers are presented. The Rayleigh number is maintained at $Ra = 3.4 \times 10^5$, and three Prandtl numbers are considered, i.e. $Pr = 12.5$ (Glycerin), $Pr = 6.8$ (Water) and $Pr = 0.025$ (Mercury). All computations were carried out on the 96×480 grid described above and the time steps for each Prandtl number were $\Delta t = 5 \times 10^{-2}$, 4×10^{-2} and 2×10^{-3}, respectively for $Pr = 12.5$, 6.8 and 0.025. The flow is steady for both cases $Pr = 12.5$ and 6.8 and unsteady for $Pr = 0.025$. For this Prandtl number, the phase portrait of Figure 4

DOI: 10.1002/cnm

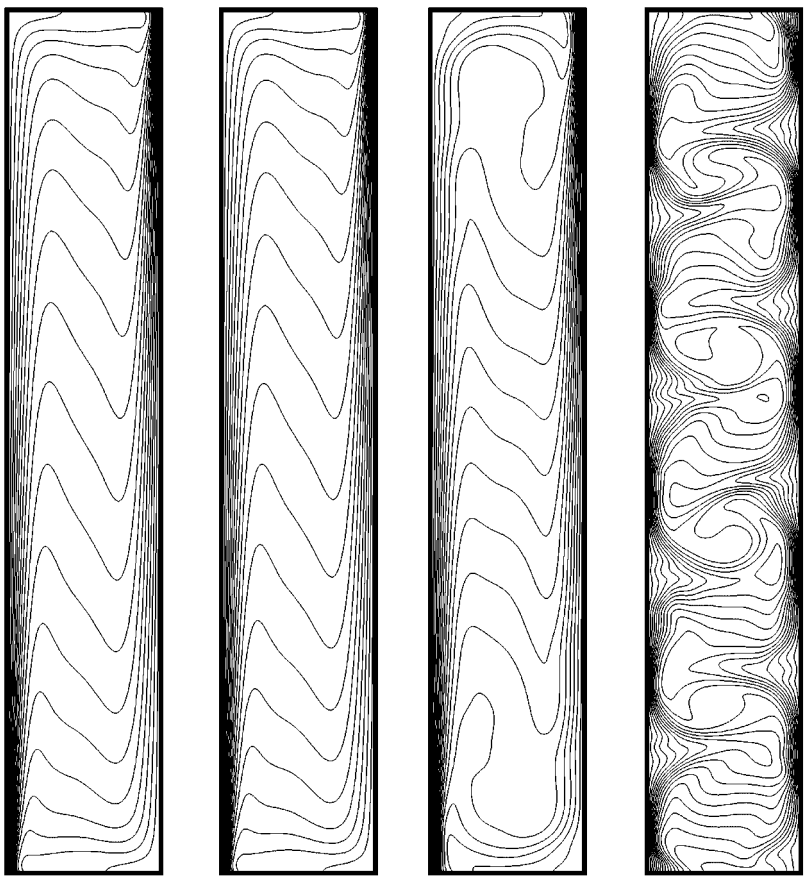

Figure 6. Temperature isolines for decreasing Prandtl numbers on grid 96×480: (a) $Pr = 12.5$; (b) $Pr = 6.8$; (c) $Pr = 0.71$; and (d) $Pr = 0.025$.

corresponding to $1420 \leqslant t \leqslant 1500$ clearly shows the presence of several frequencies in the spectrum which indicates that the regime is chaotic. The isolines of Figure 5 for the stream-function and Figure 6 for the temperature illustrate the increasing of vortex dynamics when the Prandtl number decreases. In Figure 7 is plotted the average Nusselt number *versus* the investigated Prandtl numbers. The value increases from the value 4.581 for the periodic solution of $Pr = 0.71$ to the values 4.783, 4.684 and 4.693 for the three other solutions of $Pr = 0.025$, 6.8 and 12.5, respectively. Hence, beyond the four considered Prandtl numbers, the heat transfer rate is minimum for $Pr = 0.71$ and maximum for $Pr = 0.025$.

5. CONCLUSION

The main features of an AFMG method for the solution of an 8:1 differentially heated enclosure have been presented. The performed test calculations demonstrate the potential of the MG technique

DOI: 10.1002/cnm

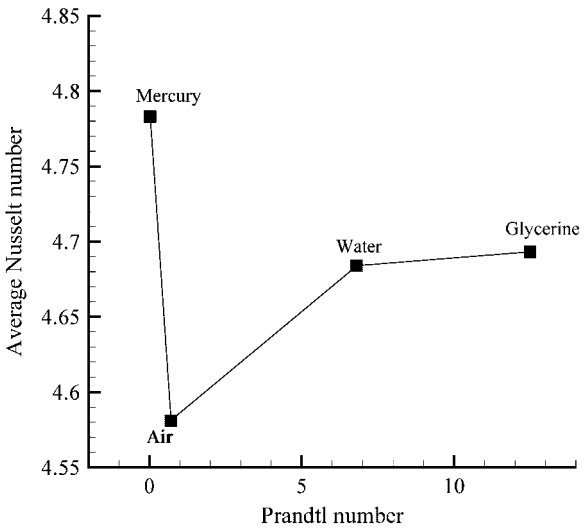

Figure 7. Average Nusselt number *versus* Prandtl number.

for enabling accurate solutions. It has also proven to be a good acceleration technique for both steady and unsteady flows. The method has been applied to study effects of Prandtl number in a tall cavity of aspect ratio $A = 8$. Three different regimes are observed at $Ra = 3.4 \times 10^5$: a steady state for $Pr = 12.5$ and 6.8, a periodic state for $Pr = 0.71$ and a chaotic state for $Pr = 0.025$. Comparing with the classical FMG method ($\Gamma = 1.0$), the AFMG method ($\Gamma = 3.75$) is more efficient. An improvement factor of $\gamma = 1.74$ is observed between the two methods. Comparing with the RBSOR scheme, the AFMG method can reach speed-up in the CPU time up to 251 times, depending on the mesh size.

REFERENCES

1. Hackbusch W. *Multigrid Methods and Applications*. Springer: Berlin, 1985.
2. Hortmann M, Peric M, Scheuerer G. Finite volume multigrid prediction of laminar natural convection: bench-mark solutions. *International Journal for Numerical Methods in Fluids* 1990; **11**:189–207.
3. Mesquita MS, De Lemos MJS. Optimal multigrid solutions of two-dimensional convection–conduction problems. *Applied Mathematics and Computation* 2004; **152**:725–742.
4. Wright NG, Gaskell PH, Sleigh PA. Natural convection in a shallow laterally heated air-filled cavity. *Communications in Numerical Methods in Engineering* 1995; **11**:937–950.
5. Stüben K. A review of algebraic multigrid. *Journal of Computational and Applied Mathematics* 2001; **128**: 281–309.
6. Braess D. Towards algebraic multigrid for elliptic problems of second order. *Computing* 1995; **55**:379–393.
7. Christon MA, Gresho PM, Sutton SB. Computational predictability of time-dependent natural convection flows in enclosures (including a benchmark solution). *International Journal for Numerical Methods in Fluids* 2002; **40**:953–980.
8. Leonard BP. A stable and accurate convective modelling procedure based on quadratic upstream interpolation. *Computer Methods in Applied Mechanics and Engineering* 1979; **19**:59–98.
9. Peyret R, Taylor TD. *Methods for Fluid Flow*. Springer: Berlin, 1983.
10. Achdou Y, Guermond JL. Convergence analysis of a finite element projection/Lagrange–Galerkin method for the incompressible Naviers–Stokes equations. *SIAM Journal on Numerical Analysis* 2000; **37**:799–826.

DOI: 10.1002/cnm